2014 International Joint Conference on Neural Networks (IJCNN)
July 6-11, 2014, Beijing, China

Kernel Canonical Variate Analysis based Management System for Monitoring and Diagnosing Smart Homes

Andrea Giantomassi, Francesco Ferracuti, Sabrina Iarlori, Sauro Longhi, Alessandro Fonti and Gabriele Comodi

***Abstract*—In the contest of household energy management, a growing interest is addressed to smart system development, able to monitor and manage resources in order to minimize wasting. One of the key factors in curbing energy consumption in the household sector is the amendment of occupant erroneous behaviours and systems malfunctioning, due to the lack of awareness of the final user. Indeed the benefits achievable with energy efficiency could be either amplified or neutralized by, respectively, good or bad practices carried out by the final users. Authors propose a diagnostic system for home energy management application able to detect faults and occupant behaviours. In particular a nonlinear monitoring method, based on Kernel Canonical Variate Analysis, is developed. To remove the assumption of normality, Upper Control Limits are derived from the estimated Probability Density Function through Kernel Density Estimation. The proposed method is applied to smart home temperature sensors to detect anomalies respect to efficient user behaviours and sensors and actuators faults. The method is tested on experimental data acquired in a real apartment.**

I. Introduction

The household sector has a wide and undeveloped potential for energy saving if compared with the tertiary or industrial sector. In most countries, nowadays the household sector is one of the biggest aggregate consumers and this is the reason why, in recent years, increasingly policies have been considering it: the sum of a high number of small energy saving actions could represent a large energy saving if considered as a whole. One of the key factors in curbing energy consumption in the household sector, together with energy efficiency and renewable energies, is widely recognized to be the amendment of occupant erroneous behaviour and systems malfunctioning, mainly explained by the lack of awareness of the final user. Indeed, energy efficiency is only one side of the household consumption charge; the other side is the occupant behaviour since the benefits achievable with energy efficiency could be either amplified or neutralized by, respectively, good or bad practices carried out by the final users [1], [2]. Furthermore, it is important to stress two considerations: first, a public utility cannot afford to pay much to affect one consumer's behaviour, yet it is only by affecting each consumer that the system can be changed [3]; second, it is important to point out that often the final user bad practices are driven by lack of unawareness or ignorance rather than bad faith, so that, training the final user with respect to energy awareness, can be more effective and cheaper than other policies [4]. In this context, energy management in homes is playing, and will play even more in future, a key role in increasing the final consumer awareness towards its own energy consumption and consequently in bursting its active role in smart grids. Also, the keyword for energy management systems is information: more accurate and more timely information. For this reason, the preliminary problem to face is the quality of the available data. The aim of this work is to propose a diagnostic system for home energy management application which, first of all, is able (i) to detect sensors and actuators malfunctioning and then is able to increase user awareness through (ii) detection of occupant bad behaviours.

Diagnostic systems are classified as model-based, signal-based and knowledge-based [5]. A signal-based approach is used in this work, to address Fault Detection and Isolation (FDI) in a Smart Home with a minimum set of sensors, it is preferred due to the monitoring system generalization capability, that allows its application to a class of systems using only a set of measurement without computing model parameters. A class of signal-based FDI methods is composed by statistical methods, which are able to reduce the correlations between variables and the dimensionality of the data [6]. These characteristics enable efficient extraction of the relevant information from the data [7], [8].

Widely applied process monitoring techniques like the Principal Component Analysis (PCA) and the Partial Least Square (PLS) rely on static models, which assume that the observations are time independent and follow a Gaussian distribution. However, the assumptions of time-independence and normality are invalid for most systems because variables driven by noise and disturbances are strongly autocorrelated and most processes are nonlinear in nature [9]. To extend PCA applications to dynamic systems, Ku *et al.* [10] presented a study of PCA on lagged variables to develop dynamic models and Multivariate Statistical Process Monitoring (MSPM) tools, called Dynamic PCA (DPCA). Principal components extracted in this way are not necessarily the minimal dynamic representation [11]. In similar way the PLS is extended to the Dynamic PLS (DPLS), with same drawbacks.

Canonical Variate Analysis (CVA), introduced in 1936 by Hotelling [12], have been developed with Upper Control Limit (UCL) based on the Gaussian assumption. Recently numerical Probability Density Function (PDF) estimation techniques are introduced for UCL where Gaussian assumption is not recognized [9], [13].

Statistical model based on CVA shows good performance and it is well known that the CVA accuracy is improved with an increase in the time lag of the data employed for the CVA analysis. However, an increment in the number of time lags can produce overfitting in the model. To address this issue and improve CVA performance a Kernel implementation of CVA

A. Giantomassi, F. Ferracuti, S. Iarlori and S. Longhi are with the Dipartimento di Ingegneria dell'Informazione, Università Politecnica delle Marche, 60131 Ancona, Italy, e-mail: {a.giantomassi, f.ferracuti, s.iarlori, sauro.longhi}@univpm.it

A. Fonti and G. Comodi are with the Dipartimento di Ingegneria Industriale e Scienze Matematiche, Università Politecnica delle Marche, 60131 Ancona, Italy, e-mail: {a.fonti, g.comodi}@univpm.it

model is proposed. CVA algorithm, extended with the kernel method, has received only a limited attention in literature, however the Kernel extension to the Canonical Correlation Analysis (CCA) is known in machine learning and pattern recognition fields [14], [15].

Kernel Canonical Variate Analysis (KCVA) is a nonlinear extension of CVA built to allow features with nonlinear dependence between variables. The basic idea of KCVA is to map the input space into a feature space via nonlinear mapping and then to compute the output space in that feature space. The main advantage of KCVA is that does not involve nonlinear optimization [16], it essentially requires only linear algebra and the solution of an eigenvalue problem. KCVA has shown better performance than CVA and Kernel PCA (KPCA) in feature extraction of nonlinear systems, but the drawback is that all kernel extensions do not provide any method for reconstructing the data in the feature space [16].

KCVA is used to compute the symptom, which means the statistical control limit that measures the fit between input data and the model trained for KCVA. UCL is computed on training dataset using the Kernel Density Estimation (KDE) to overcome normality distribution hypothesis. When residuals computed on input data exceeds the UCL then an anomaly is detected and its contributions are computed. In this way the KCVA input signals weight to each residual is obtained and the anomaly signature is identified.

The paper is organized as follows: Section II explains the basic theory of CVA model and its link with the more general Canonical Correlation Analysis (CCA). Section III presents the Kernel extension to the CVA. Section IV describes the generation of UCLs and the KDE method. Section V describes the FD procedure by KCVA with KDE UCL implemented, while experimental results are reported in Section VI. Paper ends with some considerations in Section VII.

II. Recall on CVA theory

CVA is based on the so called subspace identification [14], [17], where the process measurements are stacked to form the past and future spaces through the past $\boldsymbol{p}_t$ and future $\boldsymbol{f}_t$ observations defined as follows:

$$\boldsymbol{p}_t = \begin{bmatrix} \boldsymbol{y}_{t-q} \\ \boldsymbol{y}_{t-q+1} \\ \cdots \\ \boldsymbol{y}_{t-1} \\ \boldsymbol{u}_{t-q} \\ \boldsymbol{u}_{t-q+1} \\ \cdots \\ \boldsymbol{u}_{t-1} \end{bmatrix} \in \mathbb{R}^{q(m+r)}, \boldsymbol{f}_t = \begin{bmatrix} \boldsymbol{y}_{t} \\ \boldsymbol{y}_{t+1} \\ \cdots \\ \boldsymbol{y}_{t+q-1} \\ \boldsymbol{u}_{t} \\ \boldsymbol{u}_{t+1} \\ \cdots \\ \boldsymbol{u}_{t+q-1} \end{bmatrix} \in \mathbb{R}^{q(m+r)}, \tag{1}$$

where q is the number of lags included in the vectors. Defining N the number of input and output samples:

$$\begin{aligned} \boldsymbol{X}_p &= [\boldsymbol{p}_{q+1} \quad \boldsymbol{p}_{q+2} \quad \cdots \quad \boldsymbol{p}_{N-q+1}] \\ \boldsymbol{X}_f &= [\boldsymbol{f}_{q+1} \quad \boldsymbol{f}_{q+2} \quad \cdots \quad \boldsymbol{f}_{N-q+1}]. \end{aligned} \tag{2}$$

It is possible to define a truncated version of past and future vectors with $M \leq N - 2q + 1$ the truncated value of past and future observations . Defining the centred past and future matrices as $\tilde{\boldsymbol{X}}_p = \boldsymbol{X}_p - \bar{\boldsymbol{X}}_p$ and $\tilde{\boldsymbol{X}}_f = \boldsymbol{X}_f - \bar{\boldsymbol{X}}_f$, with $\bar{\boldsymbol{X}}_p$ and $\bar{\boldsymbol{X}}_f$ the sample means of the past and future observations, the covariance of the past, future and cross-covariance matrices are estimated as follows:

$$\boldsymbol{\Sigma} = E\left[\begin{pmatrix} \tilde{\boldsymbol{X}}_p \\ \tilde{\boldsymbol{X}}_f \end{pmatrix} \begin{pmatrix} \tilde{\boldsymbol{X}}_p \\ \tilde{\boldsymbol{X}}_f \end{pmatrix}^T\right] = \begin{pmatrix} \boldsymbol{\Sigma}_{pp} & \boldsymbol{\Sigma}_{pf} \\ \boldsymbol{\Sigma}_{fp} & \boldsymbol{\Sigma}_{ff} \end{pmatrix}, \tag{3}$$

where $\boldsymbol{\Sigma}_{ij} = \tilde{\boldsymbol{X}}_i \tilde{\boldsymbol{X}}_j^T/(M-1)$, with $i, j \in (p, f)$ [16].
Defining $\boldsymbol{c} = \boldsymbol{J}\boldsymbol{X}_p$ and $\boldsymbol{d} = \boldsymbol{L}\boldsymbol{X}_f$ the canonical variables, the goal of the CVA is to find the best linear combinations $\boldsymbol{J}$ and $\boldsymbol{L}$ of the past and future observations so that the correlation between the canonical variables is maximized. The correlation can be represented as:

$$\rho(\boldsymbol{J}, \boldsymbol{L}) = \max_{\boldsymbol{J},\boldsymbol{L}} corr(\boldsymbol{c}, \boldsymbol{d}) \tag{4}$$

$$\rho(\boldsymbol{J}, \boldsymbol{L}) = \max_{\boldsymbol{J},\boldsymbol{L}} \frac{cov(\boldsymbol{c}, \boldsymbol{d})}{var(\boldsymbol{c})^{1/2} var(\boldsymbol{d})^{1/2}} \tag{5}$$

$$\rho(\boldsymbol{J}, \boldsymbol{L}) = \max_{\boldsymbol{J},\boldsymbol{L}} \frac{\boldsymbol{J}\boldsymbol{\Sigma}_{pf}\boldsymbol{L}^T}{(\boldsymbol{J}\boldsymbol{\Sigma}_{pp}\boldsymbol{J}^T)^{1/2}(\boldsymbol{L}\boldsymbol{\Sigma}_{ff}\boldsymbol{L}^T)^{1/2}}. \tag{6}$$

If $\boldsymbol{g} = \boldsymbol{\Sigma}_{pp}^{1/2}\boldsymbol{J}^T$ and $\boldsymbol{v} = \boldsymbol{\Sigma}_{ff}^{1/2}\boldsymbol{L}^T$, the optimization problem can be defined as:

$$\begin{aligned} &\max_{\boldsymbol{g},\boldsymbol{v}} \boldsymbol{g}^T(\boldsymbol{\Sigma}_{pp}^{-1/2}\boldsymbol{\Sigma}_{pf}\boldsymbol{\Sigma}_{ff}^{-1/2})\boldsymbol{v} \\ &s.t. \quad \boldsymbol{g}^T\boldsymbol{g} = 1 \\ &\qquad \boldsymbol{v}^T\boldsymbol{v} = 1. \end{aligned} \tag{7}$$

Eq. (7) shows that CVA is equivalent to a singular value decomposition (SVD), so the solution of this problem can be obtained through the singular value decomposition (SVD):

$$\boldsymbol{\Sigma}_{pp}^{-1/2}\boldsymbol{\Sigma}_{pf}\boldsymbol{\Sigma}_{ff}^{-1/2} = \boldsymbol{G}\boldsymbol{S}\boldsymbol{V}^T, \tag{8}$$

where $\boldsymbol{G} = [\boldsymbol{g}_1, \boldsymbol{g}_2, \cdots, \boldsymbol{g}_{q(m+r)}] \in \mathbb{R}^{q(m+r)}$ and $\boldsymbol{V} = [\boldsymbol{v}_1, \boldsymbol{v}_2, \cdots, \boldsymbol{v}_{q(m+r)}] \in \mathbb{R}^{q(m+r)}$. It follows that:

$$\begin{aligned} \boldsymbol{S} &= \begin{bmatrix} \gamma_1 & 0 & \cdots & 0 \\ 0 & \gamma_2 & \cdots & 0 \\ \vdots & \vdots & \ddots & \vdots \\ 0 & 0 & \cdots & \gamma_{q(m+r)} \end{bmatrix} \\ \boldsymbol{J}\boldsymbol{\Sigma}_{pp}\boldsymbol{J}^T &= \boldsymbol{I} \\ \boldsymbol{L}\boldsymbol{\Sigma}_{ff}\boldsymbol{L}^T &= \boldsymbol{I}, \end{aligned} \tag{9}$$

with γ_i, $i = 1, \cdots, q(m+r)$, the canonical correlations and $\boldsymbol{I} \in \mathbb{R}^{q(m+r)}$ the identity matrix.

A. CVA and CCA

From the correlation coefficient defined in Eq. (4) is clear that CVA is related to the Canonical Correlation Analysis (CCA), but while both CCA and CVA are suitable for correlating two sets of variables, CVA has been applied on time series data, especially for process monitoring algorithm [18]. Then CVA can be solved as a CCA problem, hence differentiating the Eq. (6) with respect to $\boldsymbol{J}$, $\boldsymbol{L}$ and then setting the results equal to zero yields:

$$\begin{cases} \frac{\partial\rho(\boldsymbol{J},\boldsymbol{L})}{\partial\boldsymbol{J}} = \boldsymbol{\Sigma}_{pf}\boldsymbol{L}^T - 2\boldsymbol{\lambda}_1\boldsymbol{\Sigma}_{pp}\boldsymbol{J}^T = 0 \\ \frac{\partial\rho(\boldsymbol{J},\boldsymbol{L})}{\partial\boldsymbol{L}} = \boldsymbol{\Sigma}_{fp}\boldsymbol{J}^T - 2\boldsymbol{\lambda}_2\boldsymbol{\Sigma}_{ff}\boldsymbol{L}^T = 0. \end{cases} \tag{10}$$

The system in (10) can be written as the follow generalized eigenvalue problem:

$$\begin{pmatrix} \mathbf{0} & \boldsymbol{\Sigma}_{pf} \\ \boldsymbol{\Sigma}_{fp} & \mathbf{0} \end{pmatrix} \begin{pmatrix} \boldsymbol{J} \\ \boldsymbol{L} \end{pmatrix} = \boldsymbol{\lambda} \begin{pmatrix} \boldsymbol{\Sigma}_{pp} & \mathbf{0} \\ \mathbf{0} & \boldsymbol{\Sigma}_{ff} \end{pmatrix} \begin{pmatrix} \boldsymbol{J} \\ \boldsymbol{L} \end{pmatrix}$$
$$\boldsymbol{W} = \begin{bmatrix} \boldsymbol{J} \\ \boldsymbol{L} \end{bmatrix} \Rightarrow \boldsymbol{AW} = \boldsymbol{\lambda BW}. \tag{11}$$

If $\boldsymbol{\Sigma}_{pp}$ is invertible, the problem in (11) can be represented as:

$$\begin{cases} \boldsymbol{J} = \frac{1}{\boldsymbol{\lambda}} \boldsymbol{\Sigma}_{pp}^{-1} \boldsymbol{\Sigma}_{pf} \boldsymbol{L} \\ \boldsymbol{\Sigma}_{fp} \boldsymbol{\Sigma}_{pp}^{-1} \boldsymbol{\Sigma}_{pf} \boldsymbol{L} = \boldsymbol{\lambda}^2 \boldsymbol{\Sigma}_{ff} \boldsymbol{L}. \end{cases} \tag{12}$$

Solving the second equation in (12) as a generalized eigenvalue problem to obtain $\boldsymbol{L}$ and then plug the result into the first equation to receiving $\boldsymbol{J}$.

III. KERNEL CVA

Basically, Kernel CVA (KCVA) maps the data into the high dimensional space for linear separation. The nonlinear version of CVA assumes a nonlinear transformation, $\Phi_1 : \mathbb{R}^{q(m+r)} \to H_1$, of one set of input data, $\boldsymbol{X}_p \in \mathbb{R}^{q(m+r)}$ and another nonlinear transformation $\Phi_2 : \mathbb{R}^{q(m+r)} \to H_2$, of a second set of input data, $\boldsymbol{X}_f \in \mathbb{R}^{q(m+r)}$, where $\boldsymbol{X}_p$, $\boldsymbol{X}_f$ are the data series matrices containing the information from the past and future, with $M \leq N - 2q + 1$ samples and H_i, called the feature space, could have an arbitrarily large, possibly infinite, dimensionality. Then, the goal is to find $f_1 \in H_1$ and $f_2 \in H_2$ such that $f_1(\boldsymbol{X}_p) = \langle \Phi_1(\boldsymbol{X}_p), f_1 \rangle$ and $f_2(\boldsymbol{X}_f) = \langle \Phi_2(\boldsymbol{X}_f), f_2 \rangle$ have maximal correlation. For the properties of reproducing kernel Hilbert spaces (RKHS), f_1 and f_2 lie in the linear space, S_1 and S_2 respectively, which are spanned by the images of Φ_1, Φ_2. Hence:

$$\begin{aligned} f_1 &= \textstyle\sum_{i=1}^M \beta_{1i} \Phi_1(\boldsymbol{X}_{p,i}) + f_1^\perp \\ f_2 &= \textstyle\sum_{i=1}^M \beta_{2i} \Phi_2(\boldsymbol{X}_{f,i}) + f_2^\perp, \end{aligned} \tag{13}$$

where $f_1^\perp$ and $f_2^\perp$ are orthogonal to S_1 and S_2 respectively. It follows that:

$$\begin{aligned} f_1(\boldsymbol{X}_p) &= \textstyle\sum_{i=1}^M \beta_{1i} \left\langle \Phi_1(\boldsymbol{X}_p), \Phi_1(\boldsymbol{X}_{p,i}) \right\rangle \\ f_2(\boldsymbol{X}_f) &= \textstyle\sum_{i=1}^M \beta_{2i} \left\langle \Phi_2(\boldsymbol{X}_f), \Phi_2(\boldsymbol{X}_{f,i}) \right\rangle. \end{aligned} \tag{14}$$

Writing the Eq. 5 for the kernel CVA as:

$$\rho(\boldsymbol{\beta}_1, \boldsymbol{\beta}_2) = \max_{\boldsymbol{\beta}_1, \boldsymbol{\beta}_2} \frac{cov(f_1(\boldsymbol{X}_p), f_2(\boldsymbol{X}_f))}{var(f_1(\boldsymbol{X}_p))^{1/2} var(f_2(\boldsymbol{X}_f))^{1/2}}, \tag{15}$$

with:

$$\begin{aligned} \boldsymbol{\beta}_1 &= [\beta_{11}, \beta_{12}, \cdots, \beta_{1M}]^T \\ \boldsymbol{\beta}_2 &= [\beta_{21}, \beta_{22}, \cdots, \beta_{2M}]^T \end{aligned} \tag{16}$$

and defining:

$$\begin{aligned} &cov(f_1(\boldsymbol{X}_p), f_2(\boldsymbol{X}_f)) = M^{-1} \textstyle\sum_{i=1}^M f_1(\boldsymbol{X}_{p,i}) f_2(\boldsymbol{X}_{f,i}) = \\ &= M^{-1} \textstyle\sum_{i=1}^M \left\langle \Phi_1(\boldsymbol{X}_{ip}), f_1 \right\rangle \left\langle \Phi_2(\boldsymbol{X}_{if}), f_2 \right\rangle = \\ &= M^{-1} \textstyle\sum_{i=1}^M \sum_{j=1}^M \sum_{k=1}^M \beta_{1j} K_p(\boldsymbol{X}_{p,i}, \boldsymbol{X}_{p,j}) \times \\ &\times K_f(\boldsymbol{X}_{f,i}, \boldsymbol{X}_{f,k})^T \beta_{2k}^T = \\ &= M^{-1} \boldsymbol{\beta}_1 \boldsymbol{K}_p \boldsymbol{K}_f^T \boldsymbol{\beta}_2^T \end{aligned} \tag{17}$$

with:

$$\begin{aligned} var(f_1(\boldsymbol{X}_p)) &= M^{-1} \boldsymbol{\beta}_1 \boldsymbol{K}_p \boldsymbol{K}_p^T \boldsymbol{\beta}_1^T \\ var(f_2(\boldsymbol{X}_f)) &= M^{-1} \boldsymbol{\beta}_2 \boldsymbol{K}_f \boldsymbol{K}_f^T \boldsymbol{\beta}_2^T, \end{aligned} \tag{18}$$

the optimization problem (15) becomes:

$$\rho(\boldsymbol{\beta}_1, \boldsymbol{\beta}_2) = \max_{\boldsymbol{\beta}_1, \boldsymbol{\beta}_2} \frac{\boldsymbol{\beta}_1 \boldsymbol{K}_p \boldsymbol{K}_f^T \boldsymbol{\beta}_2^T}{(\boldsymbol{\beta}_1 \boldsymbol{K}_p \boldsymbol{K}_p^T \boldsymbol{\beta}_1^T)^{1/2} (\boldsymbol{\beta}_2 \boldsymbol{K}_f \boldsymbol{K}_f^T \boldsymbol{\beta}_2^T)^{1/2}}, \tag{19}$$

where $\boldsymbol{K}_p$, $\boldsymbol{K}_f$ are the Gram (or kernel) matrices, $\boldsymbol{K} : \mathbb{R}^M \times \mathbb{R}^M \to \mathbb{R}$ defined as:

$$\begin{aligned} \boldsymbol{K}_{ij} = \boldsymbol{K}(\boldsymbol{X}_i, \boldsymbol{X}_j) &= \left\langle \Phi(\boldsymbol{X}_i), \Phi(\boldsymbol{X}_j) \right\rangle \\ \boldsymbol{K} &= \left\langle \Phi(\boldsymbol{X}), \Phi(\boldsymbol{X}) \right\rangle \end{aligned} \tag{20}$$

$$\begin{aligned} \boldsymbol{K}_p &= \left\langle \Phi_1(\boldsymbol{X}_p), \Phi_1(\boldsymbol{X}_p) \right\rangle \\ \boldsymbol{K}_f &= \left\langle \Phi_2(\boldsymbol{X}_f), \Phi_2(\boldsymbol{X}_f) \right\rangle. \end{aligned} \tag{21}$$

Then Kernel CVA can be solved as a CCA problem, hence differentiating the Eq. (19) with respect to $\boldsymbol{\beta}_1$, $\boldsymbol{\beta}_2$ and then setting the results equal to zero yields:

$$\begin{cases} \frac{\partial \rho(\boldsymbol{\beta}_1, \boldsymbol{\beta}_2)}{\partial \boldsymbol{\beta}_1} = \boldsymbol{K}_p \boldsymbol{K}_f^T \boldsymbol{\beta}_2^T - 2\boldsymbol{\lambda}_1 \boldsymbol{K}_p \boldsymbol{K}_p^T \boldsymbol{\beta}_1^T = 0 \\ \frac{\partial \rho(\boldsymbol{\beta}_1, \boldsymbol{\beta}_2)}{\partial \boldsymbol{\beta}_2} = \boldsymbol{K}_f \boldsymbol{K}_p^T \boldsymbol{\beta}_1^T - 2\boldsymbol{\lambda}_2 \boldsymbol{K}_f \boldsymbol{K}_f^T \boldsymbol{\beta}_2^T = 0. \end{cases} \tag{22}$$

The above system can be written as the follow generalized eigenvalue problem:

$$\begin{pmatrix} \mathbf{0} & \boldsymbol{K}_p \boldsymbol{K}_f^T \\ \boldsymbol{K}_f \boldsymbol{K}_p^T & \mathbf{0} \end{pmatrix} \begin{pmatrix} \boldsymbol{\beta}_1 \\ \boldsymbol{\beta}_2 \end{pmatrix} = \boldsymbol{\lambda} \begin{pmatrix} \boldsymbol{K}_p \boldsymbol{K}_p^T & \mathbf{0} \\ \mathbf{0} & \boldsymbol{K}_f \boldsymbol{K}_f^T \end{pmatrix} \begin{pmatrix} \boldsymbol{\beta}_1 \\ \boldsymbol{\beta}_2 \end{pmatrix}$$
$$\boldsymbol{W} = \begin{bmatrix} \boldsymbol{\beta}_1 \\ \boldsymbol{\beta}_2 \end{bmatrix} \Rightarrow \boldsymbol{AW} = \boldsymbol{\lambda BW}. \tag{23}$$

If $\boldsymbol{K}_p \boldsymbol{K}_p^T$ is invertible, the problem in (23) can be represented as:

$$\begin{cases} \boldsymbol{\beta}_1 = \frac{1}{\boldsymbol{\lambda}} (\boldsymbol{K}_p \boldsymbol{K}_p^T)^{-1} \boldsymbol{K}_p \boldsymbol{K}_f^T \boldsymbol{\beta}_2 \\ \boldsymbol{K}_f \boldsymbol{K}_p^T (\boldsymbol{K}_p \boldsymbol{K}_p^T)^{-1} \boldsymbol{K}_p \boldsymbol{K}_f^T \boldsymbol{\beta}_2 = \boldsymbol{\lambda}^2 \boldsymbol{K}_f \boldsymbol{K}_f^T \boldsymbol{\beta}_2. \end{cases} \tag{24}$$

Solving the second equation in (24) as a generalized eigenvalue problem to obtain $\boldsymbol{\beta}_1$ and then plug the result into the first equation to receiving $\boldsymbol{\beta}_2$. At least the kernel canonical variate scores are then given by:

$$\begin{aligned} f_1(\boldsymbol{X}_p) &= \boldsymbol{K}_p \boldsymbol{\beta}_1 \\ f_2(\boldsymbol{X}_f) &= \boldsymbol{K}_f \boldsymbol{\beta}_2. \end{aligned} \tag{25}$$

One problem could be that $\boldsymbol{K}_p \boldsymbol{K}_p^T$, and therefore also $\boldsymbol{B}$, will be singular because centering renders both Gram matrices, $\boldsymbol{K}_p$ and $\boldsymbol{K}_f$, singular. The solution of this problem is to apply regularization, hence $\boldsymbol{K}_p \boldsymbol{K}_p^T$ and $\boldsymbol{K}_f \boldsymbol{K}_f^T$ become $(\boldsymbol{K}_p + \delta \boldsymbol{I})(\boldsymbol{K}_p + \delta \boldsymbol{I})^T$, $(\boldsymbol{K}_f + \delta \boldsymbol{I})(\boldsymbol{K}_f + \delta \boldsymbol{I})^T$ respectively. The solution to the optimization problem with regularization is then:

$$\begin{aligned} &\begin{pmatrix} \mathbf{0} & \boldsymbol{K}_p \boldsymbol{K}_f^T \\ \boldsymbol{K}_f \boldsymbol{K}_p^T & \mathbf{0} \end{pmatrix} \begin{pmatrix} \boldsymbol{\beta}_1 \\ \boldsymbol{\beta}_2 \end{pmatrix} = \\ &= \boldsymbol{\lambda} \begin{pmatrix} \begin{matrix} (\boldsymbol{K}_p + \delta \boldsymbol{I}) \times \\ \times (\boldsymbol{K}_p + \delta \boldsymbol{I})^T \end{matrix} & \mathbf{0} \\ \mathbf{0} & \begin{matrix} (\boldsymbol{K}_f + \delta \boldsymbol{I}) \times \\ \times (\boldsymbol{K}_f + \delta \boldsymbol{I})^T \end{matrix} \end{pmatrix} \begin{pmatrix} \boldsymbol{\beta}_1 \\ \boldsymbol{\beta}_2 \end{pmatrix}. \end{aligned} \tag{26}$$

Defining the canonical variable $f_1(\boldsymbol{X}_p) = \boldsymbol{K}_p\boldsymbol{\beta}_1 \in \mathbb{R}^M$, that are uncorrelated and have unit variance, the KCVA control limit is the $\boldsymbol{T}^2$ statistic defined as:

$$\boldsymbol{T}^2 = \boldsymbol{f_1}(\boldsymbol{X_p})^T \boldsymbol{f_1}(\boldsymbol{X_p}) = \boldsymbol{\beta}_1^T \boldsymbol{K}_p^T \boldsymbol{K}_p \boldsymbol{\beta}_1. \tag{27}$$

In order to identify fault variables for the KCVA-based diagnosis, the contribution plot method is implement for the $\boldsymbol{T}^2$ monitoring statistics. Since $\boldsymbol{T} = \boldsymbol{K}_p\boldsymbol{\beta}_1 = (\boldsymbol{K}_{1p} \circ \boldsymbol{K}_{2p} \circ \cdots \circ \boldsymbol{K}_{mp})\boldsymbol{\beta}_1$, where m is the number of variables, the contribution are defined as:

$$\boldsymbol{CT_i^2} = \boldsymbol{\beta}_1^T \boldsymbol{K}_{ip}^T \boldsymbol{K}_{ip} \boldsymbol{\beta}_1. \tag{28}$$

IV. Upper Control Limit

When the normality assumption is not valid, the solution is to estimate the PDF directly for $\boldsymbol{T}^2$ through a non parametric approach. In [9], the KDE is considered because it is a well established non parametric approach to estimate the PDF of $\boldsymbol{T}^2$ statistic and evaluate the control limits $\boldsymbol{T}^2_\alpha UCL$. Assume y is a random variable and its density function is denoted by $p(y)$. This means that:

$$P(y < b) = \int_{-\infty}^{b} p(y)dy. \tag{29}$$

Hence, by knowing $p(y)$, an appropriate control limit can be determined for a specific confidence bound α, using Eq. (29). Replacing $p(y)$, in Eq. (29), with the PDF estimation of $\boldsymbol{T}^2$, called $\hat{p}(\boldsymbol{T}^2)$ the control limits will be estimated by:

$$\int_{-\infty}^{\boldsymbol{T}^2_\alpha UCL} \hat{p}(\boldsymbol{T}^2) d\boldsymbol{T}^2 = \alpha \tag{30}$$

V. KCVA based Fault Detection Algorithm

The developed Kernel CVA based Fault Detection procedure consists of two stages: the first one is related to the training step where faultless data are processed and a model of this data is built, and the second one regards the detection step where the model obtained in the previous step is used to compute on-line the fault statistics. Kernel CVA training step are summarized below:

- T1. Collect and preprocess data, define past and future data series $\boldsymbol{X}_p$, $\boldsymbol{X}_f$.
- T2. Scale $\boldsymbol{X}_p$ and $\boldsymbol{X}_f$ matrices.
- T3. Define a kernel function, with respective parameters, compute the Gram matrices $\boldsymbol{K}_p^{TR}$, $\boldsymbol{K}_f^{TR}$ with Eq. (21).
- T4. Center the Gram matrices $\boldsymbol{K}_p^{TR}$, $\boldsymbol{K}_f^{TR}$.
- T5. Calculate $\boldsymbol{\beta}_1$ by solving the eigenvalue problem in Eq. (26).
- T6. Normalize eigenvectors $\boldsymbol{\beta}_1$ so that $\boldsymbol{\beta}_1^T(\boldsymbol{K}_p^{TR})^T(\boldsymbol{K}_p^{TR})\boldsymbol{\beta}_1 = \boldsymbol{I}$, with $\boldsymbol{I}$ the identity matrix.
- T7. Calculate $\boldsymbol{T}^2$ with Eq. (27).
- T8. Estimate $\hat{p}(\boldsymbol{T}^2)$ with KDE approach and calculate the threshold $\boldsymbol{T}^2_\alpha UCL$ with Eq. (30).

The Gram matrices are centred as follows [19]:

$$\boldsymbol{K}^{TR} = \boldsymbol{K}^{TR} - \boldsymbol{1}_{TR}\boldsymbol{K}^{TR} - \boldsymbol{K}^{TR}\boldsymbol{1}_{TR} + \boldsymbol{1}_{TR}\boldsymbol{K}^{TR}\boldsymbol{1}_{TR} \tag{31}$$

with:

$$\boldsymbol{1}_{TR_{(M\times M)}} = 1/M \cdot \begin{bmatrix} 1 & \cdots & 1 \\ \vdots & \ddots & \vdots \\ 1 & \cdots & 1 \end{bmatrix}. \tag{32}$$

In the second step, called detection step, the previous model is on-line compared with the new data and a statistical index of faults is calculated. Kernel CVA detection steps are summarized below:

- D1. New data are preprocessed and the past and future data series $\boldsymbol{p}_t$, $\boldsymbol{f}_t$ are defined.
- D2. $\boldsymbol{p}_t$ and $\boldsymbol{f}_t$ vectors are scaled with the same mean and standard deviation of step T2.
- D3. With the same kernel function and its parameters defined in step T3, the Gram matrices $\boldsymbol{K}_p^{TS} = \langle \Phi_1(\boldsymbol{p}_t), \Phi_1(\boldsymbol{X}_p)\rangle$, $\boldsymbol{K}_f^{TS} = \langle \Phi_2(\boldsymbol{f}_t), \Phi_2(\boldsymbol{X}_f)\rangle$ are computed.
- D4. The Gram matrices $\boldsymbol{K}_p^{TS}$, $\boldsymbol{K}_f^{TS}$ are centred:

  $$\boldsymbol{K}^{TS} = \boldsymbol{K}^{TS} - \boldsymbol{1}_{TS}\boldsymbol{K}^{TR} - \boldsymbol{K}^{TS}\boldsymbol{1}_{TR} + \boldsymbol{1}_{TS}\boldsymbol{K}^{TR}\boldsymbol{1}_{TR}, \tag{33}$$

  with:

  $$\boldsymbol{1}_{TS_{(1\times M)}} = 1/M \cdot [1 \quad \cdots \quad 1]. \tag{34}$$

- D5. $\boldsymbol{T}^2$ is calculated with Eq. (27).
- D6. **If** $\boldsymbol{T}^2$ is over the threshold $\boldsymbol{T}^2_\alpha UCL$ the fault is detected and fault isolation is performed by the contribution plot method with Eq. (28), **else** the next data set is analyzed (return to D1).

The input parameters are q, the time lag of past and future matrices $\boldsymbol{X}_p$, $\boldsymbol{X}_f$ defined in Eq. (2), the kernel function $\Phi(\cdot)$ and the kernel function parameters.

VI. Experimental Setup and Results

The methodology proposed was tested on a real apartment occupied by a single person who works all the day (8.30-18.30) and comes back home for lunch time (12.30-14.30). The apartment has a hydronic radiant underfloor heating system, with 3 smart thermostatic valves. The apartment temperatures (see Fig. 1) were monitored for a whole winter season and the KCVA inputs are: i) rooms temperature; ii) derivative of the rooms temperature; iii) temperature difference between rooms. The analysis of data showed that the main repeated energy wasting occupant behaviour is the opening of a window while the heating system is on. Furthermore, the methodology proposed detects some recurrent behaviours which can not be exactly classified as bad occupant behaviour but which could be optimized in order to reduce the home energy consumption; in particular, the methodology points-out the role of cooking loads (oven and stoves) and human activity (ironing) free contributions to ambient temperature. The methodology detects that the room temperature of the kitchen/living room strongly exceeds the set-point room temperature during mealtimes. This is due to the fact that the thermostat was installed in another room. This situation could be optimized, for example, by lowering the set-point temperature one hour before meal time, thus reducing the thermal energy consumption of the apartment. The proposed methodology also detects the increase of temperature due to ironing. The explanation is the same of the previous event. The thermostat sensor has been installed

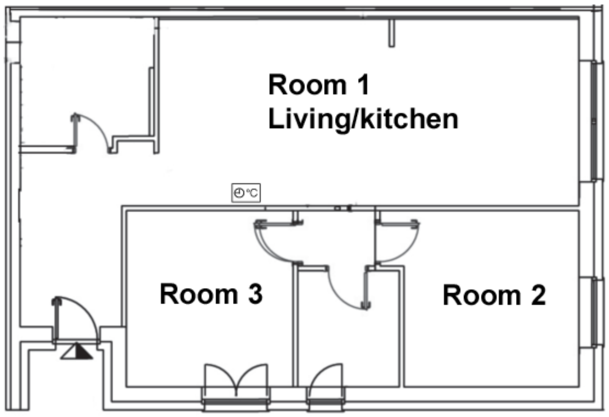

(a)

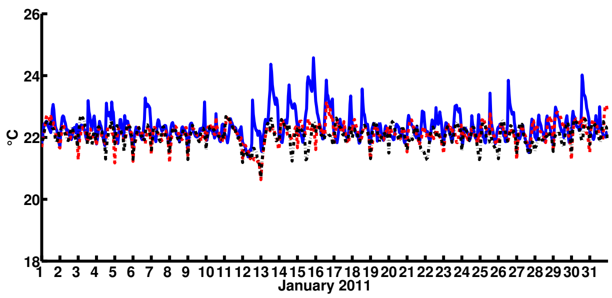

(b)

Fig. 1. a) apartment planimetry; b) temperature trend during January 2011, solid blue line refers to room 1, red dashed line refers to room 2 and black dot line refers to room 3.

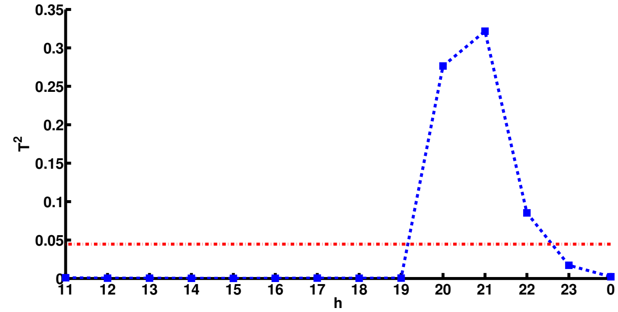

(a)

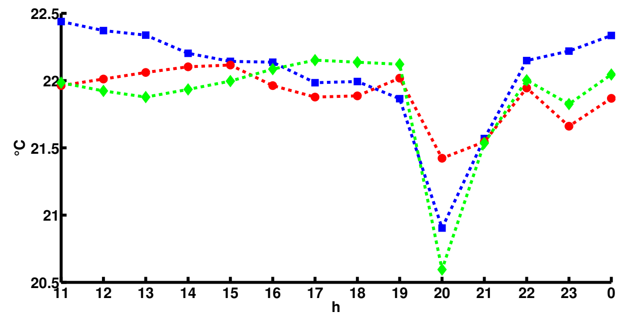

(b)

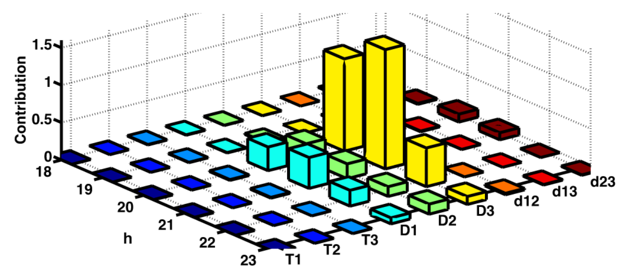

(c)

Fig. 2. Windows open behaviour; a) T^2 trend in blue dashed vs. UCL in red dotted; b) rooms temperatures, room 1 in blue squares, room 2 in red dots and room 3 in green diamonds; c) signals contributions, T_i are the rooms temperatures, D_i denote the temperatures derivatives and d_{ij} are the temperature differences.

in a different room, so the temperature in the room where the ironing happened is boosted; in the case of a smart BEMS (Building Energy Management System) being aware of the task scheduled by the occupant, the set-point temperature of the thermostat could be lowered conveniently. The monitoring methodology allows, also, to detect heating system sensors malfunction; the sensors fault detection is crucial, as stated in Sec. I, to save the heating system in top shape. Finally, the methodology was tested also to diagnose the malfunctioning of a heating system actuator, in particular a thermostatic distribution valve in one room. In this case, the fault was simulated by blocking the valve in a partially closed position.

A. *Human Behaviour*

Figs. 2 and 3 show two different results related to the diagnosis of opening windows. The first behaviour diagnosed, depicted in Figs. 2(a), 2(b), 2(c), is related to an open window for each room. It can be noted that the main contribution is given by the temperatures derivative, indeed when the heating system is on, an opening window yields an abrupt decrease in temperature and in the same way, when the window is closed, the temperature quickly recovers the gap.

Figs. 3(a), 3(b), 3(c) report that the user left the room 3 drop-front window open for all the day. The result is an evident increment in the contribution of the differences between rooms, but the bad behaviour is detected with an abrupt signal of the room 3 temperature derivative in the morning. This trend ends in the evening when the user came back home and closes the window.

The next two examples, Figs. 4 and 5 refer to the case of free contributions due to cooking. The former shows the event both at lunch and dinner time; the latter shows an event occurring during lunch time. In the first case, depicted in Figs. 4(a), 4(b) and 4(c) the derivative of temperature plays an important role in the detection of the event, also the difference of temperature detects an anomaly. In the second case, Figs. 5(a), 5(b) and 5(c), it is important to point-out that the event is identified through the temperature derivative of the living room.

The following example shows the detection of another human activity which implies an high free contribution of heat in the apartment with a consequent rise in its temperature. The Figs. 6(a), 6(b) and 6(c) show the high increase of temperature in room 2 due to ironing activity from 21.00 to 22.30 in the evening. The event was clearly detected by room 2 temperature derivative. Even if the event lasted two hours its effect on room

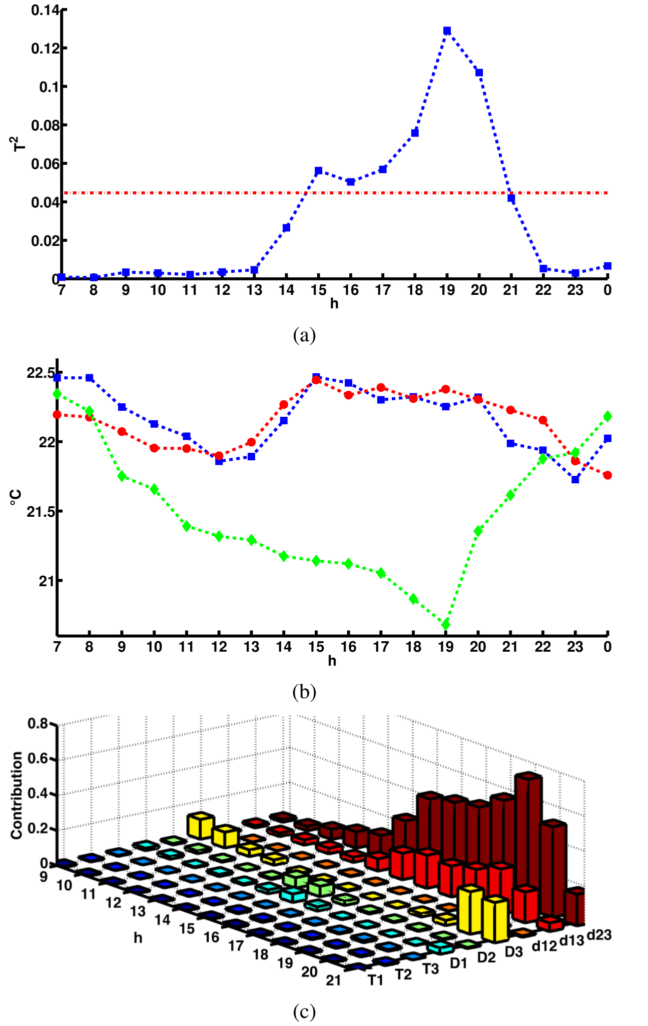

Fig. 3. Drop-front window open; a) T^2 trend in blue dashed vs. UCL in red dotted; b) rooms temperatures, room 1 in blue squares, room 2 in red dots and room 3 in green diamonds; c) signals contributions, T_i are the rooms temperatures, D_i denote the temperatures derivatives and d_{ij} are the temperature differences.

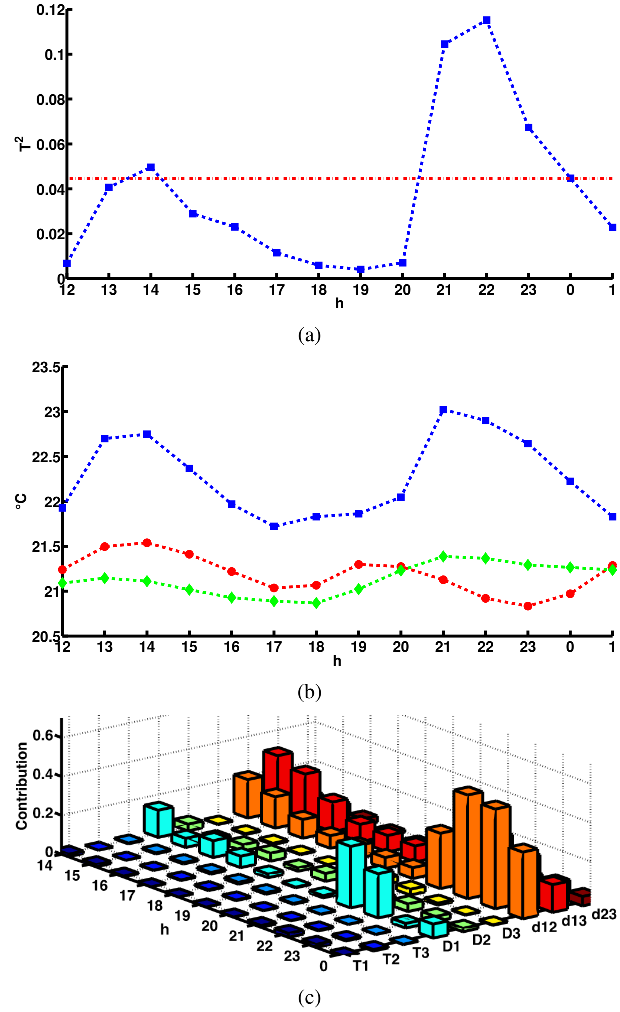

Fig. 4. Lunch and meal time behaviours; a) T^2 trend in blue dashed vs. UCL in red dotted; b) rooms temperatures, room 1 in blue squares, room 2 in red dots and room 3 in green diamonds; c) signals contributions, T_i are the rooms temperatures, D_i denote the temperatures derivatives and d_{ij} are the temperature differences.

temperature had repercussions for further three hours.

B. Heating System Malfunctions

The following Figs. 7(a), 7(b) and 7(c) show the identification of the malfunctioning of a room sensor. In this case the high contribution is clearly due to the room temperature parameter. KCVA detects that the value is out of control, than the derivative and the difference of temperature have no meaning.

The last example, showed in Figs. 8(a), 8(b) and 8(a) refers to the malfunctioning of a distribution valve of the heating system. As aforementioned, this fault is inducted in order to test the methodology proposed. For this reason the thermostatic valve in room 3 is blocked in a certain partial position so that less thermal power is provided to the room. Looking at the temperature trends, it is possible to see that the dynamic of temperature in room 3 was connected to the the trend of other room temperatures (the partition wall and doors between the rooms were not thermally insulated) but remained a couple of degree lower. The proposed methodology detects the fault, the major contributor is the difference of temperature between the other rooms and the room temperature itself.

VII. Concluding Remarks

The methodology has proved to be very powerful since it allowed to diagnose several faults simply monitoring the trend of ambient temperature of each room of the apartment. One of the main advantages of detecting more faults by monitoring just one parameter is the low price of the BEMS due to the reduced number of sensors. As an example, the methodology proposed allowed to detect an open window by real-time, monitoring the room ambient temperature without installing a contact sensor in each window. The development and validation of a signal-based diagnostic system based on KCVA is presented. The proposed implementation of KCVA method is augmented with a PDF estimator to better compute the fault thresholds. The KDE allows to deal with processes where

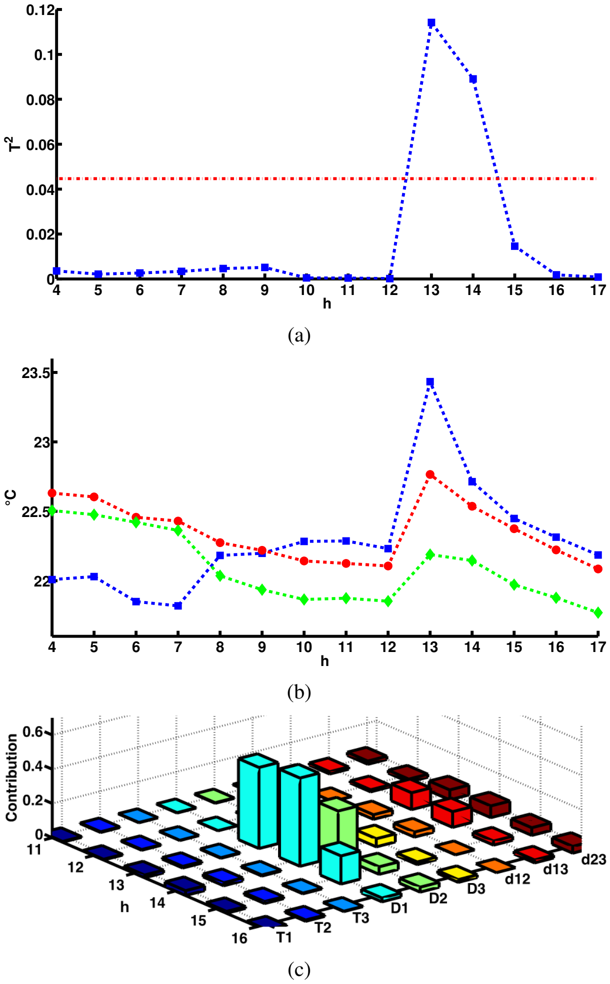

Fig. 5. Lunch behaviour; a) T^2 trend in blue dashed vs. UCL in red dotted; b) rooms temperatures, room 1 in blue squares, room 2 in red dots and room 3 in green diamonds; c) signals contributions, T_i are the rooms temperatures, D_i denote the temperatures derivatives and d_{ij} are the temperature differences.

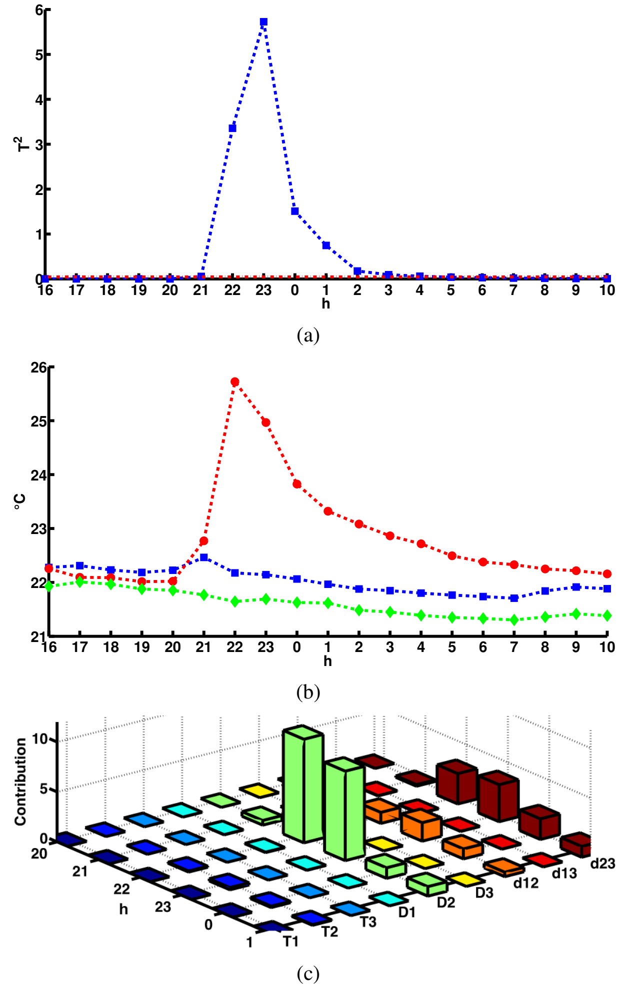

Fig. 6. Human activity; a) T^2 trend in blue dashed vs. UCL in red dotted; b) rooms temperatures, room 1 in blue squares, room 2 in red dots and room 3 in green diamonds; c) signals contributions, T_i are the rooms temperatures, D_i denote the temperatures derivatives and d_{ij} are the temperature differences.

signals do not match the Gaussian distribution hypothesis. The monitoring system by the proposed KCVA algorithm promotes the detection of faults and human behaviours in order to manage the optimal operation of the BEMS. Results highlight that KCVA, using KDE thresholds estimation, guarantees robustness and repeatability about results. Future works involve the employment of an Interactive Interface with users to give them feedbacks about bad behaviours and tips to overcome energy wasting. To improve the classification of faults and include more heating systems fault types it is possible to extend the set of sensors monitored by KCVA. A strategy involves the acquisition of the thermostatic valve position signals. Authors are developing the extension of the diagnostic method to include the cooling system for the summer season.

REFERENCES

[1] A. Faiers, M. Cook, and C. Neame, "Towards a contemporary approach for understanding consumer behaviour in the context of domestic energy use," *Energy Policy*, vol. 35, no. 8, pp. 4381 – 4390, 2007.

[2] G. Comodi, A. Giantomassi, A. Arteconi, C. Meloni, and S. Pizzuti, "Proposal of a system for diagnosing with inefficient occupant behaviour and systems malfunctioning in the household sector," in *WIT Transactions on Ecology and the Environment*, 2011, pp. 699–710.

[3] S. Hauser and K. Crandall, *Smart Grid - Integrating Renewable, Distributed & Efficient Energy*. Academic Press, 2012, ch. Smart Grid is a Lot More than Just "Technology".

[4] A. Lindén, A. Kanyama, and B. Eriksson, "Efficient and inefficient aspects of residential energy behaviour: What are the policy instruments for change?" *Energy Policy*, vol. 34, no. 14, pp. 1918 – 1927, 2006.

[5] F. Ferracuti, A. Giantomassi, S. Longhi, and N. Bergantino, "Multiscale PCA based fault diagnosis on a paper mill plant," in *Emerging Technologies Factory Automation (ETFA), 2011 IEEE 16th Conference on*, Toulouse, France, 2011, pp. 1–8.

[6] F. Ferracuti, A. Giantomassi, and S. Longhi, "MSPCA with KDE Thresholding to Support QC in Electrical Motors Production Line," in *7th IFAC Conf. on Manufacturing Modeling, Management and Control*, vol. 7, 2013.

[7] C. Ciandrini, M. Gallieri, A. Giantomassi, G. Ippoliti, and S.Longhi, "Fault detection and prognosis methods for a monitoring system of rotating electrical machines," in *IEEE International Symposium on Industrial Electronics (ISIE)*, Bari, Italy, 2010, pp. 2085–2090.

[8] F. Ferracuti, A. Giantomassi, S. Longhi, and G. Ippoliti, "Multi-scale PCA based fault diagnosis for rotating electrical machines," in *8th ACD 2010 European Workshop on Advanced Control and Diagnosis*, 2010, pp. 1–6.

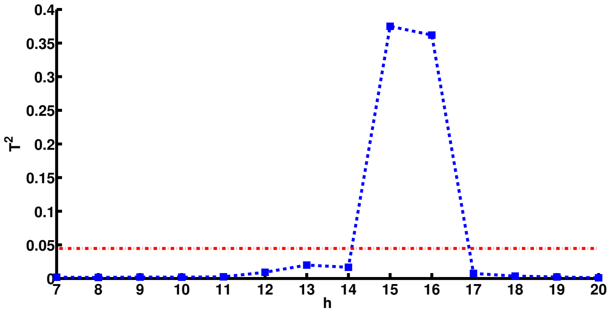

(a)

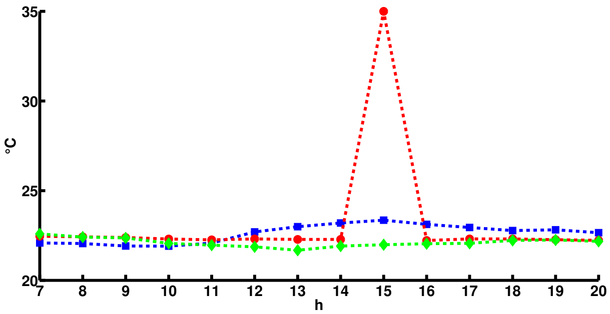

(b)

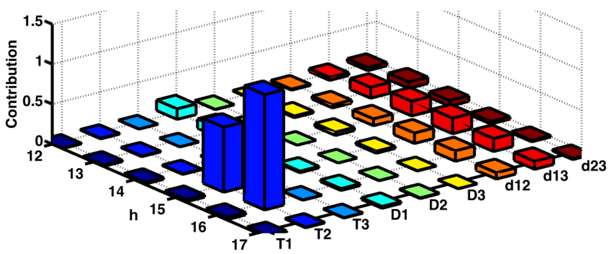

(c)

Fig. 7. Sensor malfunction; a) T^2 trend in blue dashed vs. UCL in red dotted; b) rooms temperatures, room 1 in blue squares, room 2 in red dots and room 3 in green diamonds; c) signals contributions, T_i are the rooms temperatures, D_i denote the temperatures derivatives and d_{ij} are the temperature differences.

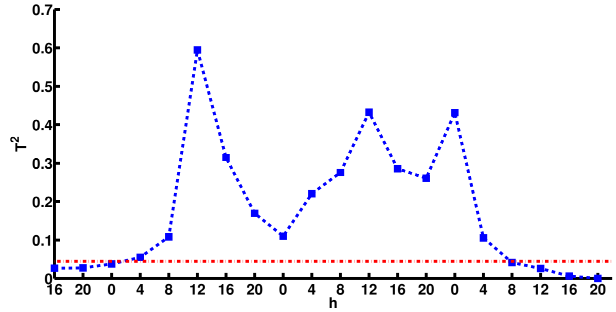

(a)

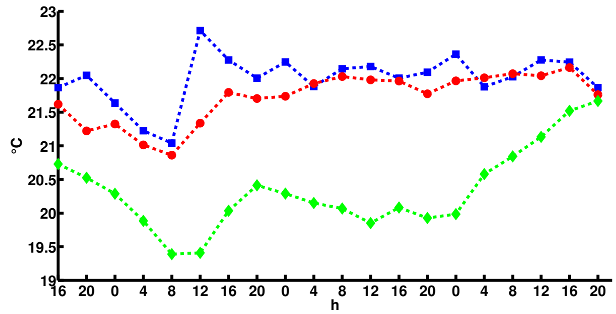

(b)

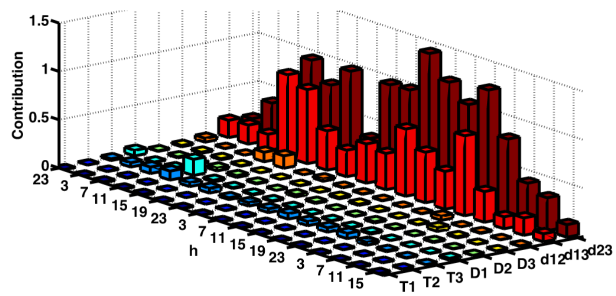

(c)

Fig. 8. Thermostatic valve malfunction; a) T^2 trend in blue dashed vs. UCL in red dotted; b) rooms temperatures, room 1 in blue squares, room 2 in red dots and room 3 in green diamonds; c) signals contributions, T_i are the rooms temperatures, D_i denote the temperatures derivatives and d_{ij} are the temperature differences.

[9] P.-E. Odiowei and Y. Cao, “Nonlinear dynamic process monitoring using canonical variate analysis and kernel density estimations,” *Industrial Informatics, IEEE Transactions on*, vol. 6, no. 1, pp. 36–45, Feb 2010.

[10] W. Ku, R. H. Storer, and C. Georgakis, “Disturbance detection and isolation by dynamic principal component analysis,” *Chemometrics and Intelligent Laboratory Systems*, vol. 30, no. 1, pp. 179 – 196, 1995.

[11] A. Negiz and A. Cinar, “Monitoring of multivariable dynamic processes and sensor auditing,” *Journal of Process Control*, vol. 8, no. 5–6, pp. 375 – 380, 1998.

[12] A. Norvilas, A. Negiz, J. DeCicco, and A. Cinar, “Intelligent process monitoring by interfacing knowledge-based systems and multivariate statistical monitoring,” *Journal of Process Control*, vol. 10, no. 4, pp. 341 – 350, 2000.

[13] F. Ferracuti, A. Giantomassi, S. Iarlori, G. Ippoliti, and S. Longhi, “Induction motor fault detection and diagnosis using KDE and Kullback-Leibler divergence,” in *Industrial Electronics Society, IECON 2013 - 39th Annual Conference of the IEEE*, 2013, pp. 2923–2928.

[14] X. Zhu, Z. Huang, H. T. Shen, J. Cheng, and C. Xu, “Dimensionality reduction by mixed kernel canonical correlation analysis,” *Pattern Recognition*, vol. 45, no. 8, pp. 3003 – 3016, 2012.

[15] S.-Y. Huang, M.-H. Lee, and C. K. Hsiao, “Nonlinear measures of association with kernel canonical correlation analysis and applications,” *Journal of Statistical Planning and Inference*, vol. 139, no. 7, pp. 2162 – 2174, 2009.

[16] B. Schölkopf and A. Smola, *Learning with Kernels*. MIT Press, 2001.

[17] L. Chiang, E. Russell, and R. Braatz, *Fault Detection and Diagnosis in Industrial Systems*. Springer, 2001.

[18] A. J. Izenman, *Modern Multivariate Statistical Techniques : Regression, Classification, and Manifold Learning*, ser. Springer Texts in Statistics. Springer New York, 2008.

[19] B. Schölkopf, A. Smola, E. Smola, and K.-R. Müller, “Nonlinear Component Analysis as a Kernel Eigenvalue Problem,” *Neural Computation*, vol. 10, pp. 1299–1319, 1998.